MAGNETIC RESONANCE IN CHEMISTRY, VOL. 35, 468–476 (1997)

New Form of Rational Function in NMR Lineshape Fitting: Application to Four Overlapping Resonances from a Three-Spin System

D. E. Roberts,[1] Y. Z. Wu,[2] R. Yusaf,[1] J. Higinbotham,[2]* A. J. Shand[1] and I. C. Malcolm[1]
[1] Department of Mathematics, Napier University, 10 Colinton Road, Edinburgh EH10 5DT, UK
[2] Department of Applied Chemical and Physical Sciences, Napier University, 10 Colinton Road, Edinburgh EH10 5DT, UK

The analyses of NMR and ESR spectra involve the accurate and fast determination of parameters such as position, width and intensity in the presence of noise. A new frequency domain method, using rational functions based on sets of orthogonal polynomials to simulate the NMR lineshape, has been developed. This method does not require any initial values for the parameters and is not restricted to a particular lineshape. It is illustrated by application to the simulated spectra of the four resonances for the C-26 and C-27 carbon atoms in the ^{13}C NMR spectrum of 16.67 mol.% [25,26,27-^{13}C]cholesterol in dimyristoylphosphatidylcholine vesicles for various noise levels and spectrometer frequencies. © **1997 by John Wiley & Sons, Ltd.**

Magn. Reson. Chem. **35**, 468–476 (1997) No. of Figures: 6 No. of Tables: 3 No. of References: 16

Keywords: NMR lineshape; rational function; orthogonal polynomials; frequency domain

Received 5 February 1996; revised 17 February 1997; accepted 18 February 1997

INTRODUCTION

The analysis of spectra, such as those from NMR and ESR, involves the accurate and fast determination of parameters such as position, width and intensity in the presence of noise. The analysis may be performed in either the time domain or the frequency domain. For magnetic resonance spectroscopy (MRS) performed *in vivo* on humans, where large baseline distortions are usually present along with low signal-to-noise (S/N) ratios, linear prediction techniques applied in the time domain have proved useful.[1] This approach has recently been extended by including the total least-squares technique to estimate the parameters.[2]

For NMR spectra, a common approach in the frequency domain is to fit the resonances in the spectrum with a linear combination of Lorentzian and Gaussian shapes using a non-linear least-squares procedure.[3] The fitting of this lineshape function can also be performed in the time domain.[4]

Accurate values of scalar coupling constants are an important aid in the determination of chemical structure. In order to determine these scalar coupling constants, it is necessary to determine accurately the positions of the associated resonances. Poorly resolved scalar interaction splittings can be measured with improved accuracy by using the signal processing technique of *J*-doubling in the frequency domain.[5] For Lorentzian lineshapes with S/N ratios >20, complex least-squares fitting in the frequency domain can be performed automatically, taking into account baseline corrections.[6]

Rational functions were introduced by Maltempo[7] for approximating two overlapping resonances having generalized spectroscopic lineshapes. These functions have two main advantages, namely of being entirely general even if the lineshape is asymmetric, and of not requiring any preliminary knowledge of parameters. More recently, Bergmann *et al.*[8] have investigated two overlapping resonances of Lorentzian shape using rational functions. In the present study we used rational functions based on sets of orthogonal polynomials. Although in principle this method may be applied to more general lineshapes, the application in the present work is also to those of the Lorentzian form. The spectra are assumed to be correctly phased so that only real data are considered.

In this paper, the details of the new method are presented. The method is then illustrated by applying it to the simulated spectrum of the four C-26 and C-27 resonances of the isopropyl group in the ^{13}C NMR spectrum of 16.67 mol.% [25,26,27-^{13}C]cholesterol in dimyristoylphosphatidylcholine (DMPC) vesicles[9] for various noise levels and spectrometer frequencies.

THEORY

This section is concerned with the presentation of an iterative method of determining a rational function which fits a given lineshape in a least-squares sense.[10] For the case of m Lorentzian lines, the degree N of the denominator is $2m$, while that of the numerator, M, is $2m-2$. In partial fraction form, the line shape, $g(x)$ is

* *Correspondence to*: J. Higinbotham.

 CCC 0749–1581/97/070468–09 $17.50

described by

$$g(x) = \sum_{k=1}^{m} \frac{A_k}{(x - \alpha_k)^2 + (\beta_k)^2} \quad (1)$$

where the *real* numbers, A_k, α_k and β_k ($k = 1, 2, \ldots, m$), are to be estimated from the fit.

From a computational point of view it is important to ensure that the problem is not ill-conditioned in order to maintain numerical stability. Therefore, in this paper an approach is proposed which combines the use of rational functions as proposed by Bergmann *et al.*[8] with the established practice of fitting polynomials to given data using orthogonal polynomial bases.[11] A system of linear equations is solved at each iteration.[8] Hence, the condition number [Eqn (29)] of this system may be used to monitor numerical stability.

The problem may be stated as follows. For the given data (x_i, f_i), $i = 1, \ldots, n$, two polynomials $P(x)$, $Q(x)$ of maximum degrees M and N, respectively, are sought such that the quantity

$$L := \sum_{i=1}^{n} \left[f_i - \frac{P(x_i)}{Q(x_i)} \right]^2 \quad (2)$$

is a minimum. In terms of the equations determining the coefficients of the numerator and denominator polynomials, this is a non-linear problem. It may be reduced, however, to a sequence of linear problems by considering the following quantities for the kth iteration:[8]

$$L^{(k)} := \sum_{i=1}^{n} W^{(k)}(x_i)[f_i Q^{(k)}(x_i) - P^{(k)}(x_i)]^2 \quad k = 1, 2, \ldots \quad (3)$$

where

$$W^{(k)}(x) := [Q^{(k-1)}(x)]^{-2} \quad (4)$$

An iteration is begun by providing a reasonable starting form for the denominator polynomial $Q^{(0)}(x)$. For example, the results presented are obtained using $Q^{(0)}(x) = 1 + x + x^2 + \cdots + x^N$. Since, at the kth iteration stage, $W^{(k)}(x)$ is known, $L^{(k)}$ may then be minimised to obtain $P^{(k)}(x)$ and $Q^{(k)}(x)$ by solving a system of *linear* equations. Termination is reached when corresponding polynomials of consecutive steps are sufficiently close to each other. There is no guarantee, however, that this will happen, although numerical experiments indicate that this is usually the case.

To make the above ideas precise, the following definitions are made:

$$P^{(k)}(x) := \sum_{j=0}^{M} a_j^{(k)} p_j^{(k)}(x) \quad k = 0, 1, \ldots \quad (5)$$

and

$$Q^{(k)}(x) := \sum_{r=0}^{N} b_r^{(k)} q_r^{(k)}(x) \quad k = 0, 1, \ldots \quad (6)$$

where the $p_j^{(k)}(x)$ and $q_r^{(k)}(x)$ are polynomials of degrees j and r, respectively, and in particular, $q_0^{(k)}(x) = p_0^{(k)}(x) = 1$ For example, we may choose $p_j^{(k)}(x) = q_j^{(k)}(x) = x^j$.[8] Just as in polynomial least-squares fitting,[11] however, this choice leads to ill-conditioning even for quite small values of M and N.

Pursuing the analogy with the simpler polynomial fit, $p_j^{(k)}(x)$ and $q_r^{(k)}(x)$ are now constructed to be two systems of polynomials, orthogonal with respect to different weight functions (see Appendix A). One system. $\{p_j^{(k)}(x): j = 0, 1, \ldots, M\}$ consists of polynomials orthogonal to each other with respect to the weight $W^{(k)}(x)$ on $\{x_1, x_2, \ldots, x_n\}$:

$$\sum_{i=1}^{n} W^{(k)}(x_i) p_j^{(k)}(x_i) p_l^{(k)}(x_i) = d_j^{(k)} \delta_{jl} \quad j, l = 0, 1, \ldots, M \quad (7)$$

where $d_j^{(k)}$ are positive numbers. The second orthogonal system $\{q_r^{(k)}(x): r = 0, 1, \ldots, N\}$ uses the weight sequence $\{f_i^2 W^{(k)}(x_i): i = 0, 1, \ldots, n\}$:

$$\sum_{i=1}^{n} f_i^2 W^{(k)}(x_i) q_r^{(k)}(x_i) q_s^{(k)}(x_i) = e_r^{(k)} \delta_{rs} \quad r, s = 0, 1, \ldots, N \quad (8)$$

where $e_r^{(k)}$ are positive numbers.

For an extremum of $L^{(k)}$, the following equations must hold:

$$\frac{\partial L^{(k)}}{\partial a_j^{(k)}} = 0 \quad j = 0, 1, \ldots, M \quad (9)$$

and

$$\frac{\partial L^{(k)}}{\partial b_r^{(k)}} = 0 \quad r = 1, 2, \ldots, N \quad (10)$$

where, in order to normalize the rational function $P^{(k)}(x)/Q^{(k)}(x)$, $b_0^{(k)}$ is set to unity. Using Eqns (3) and (5), the condition in Eqn (9) yields

$$-\sum_{i=1}^{n} W^{(k)}(x_i)[f_i Q^{(k)}(x_i) - P^{(k)}(x_i)] p_j^{(k)}(x_i) = 0 \quad j = 0, 1, \ldots, M \quad (11)$$

which may be rewritten, using Eqn (7), in matrix form:

$$D^{(k)} a^{(k)} - C^{(k)} b^{(k)} = B^{(k)} \quad (12)$$

where

$$\left.\begin{aligned} D_{jl}^{(k)} &:= \delta_{jl} \frac{1}{n} \sum_{i=1}^{n} W^{(k)}(x_i)[p_l^{(k)}(x_i)]^2 \\ C_{jr}^{(k)} &:= \frac{1}{n} \sum_{i=1}^{n} f_i W^{(k)}(x_i) q_r^{(k)}(x_i) p_j^{(k)}(x_i) \\ B_l^{(k)} &:= \frac{1}{n} \sum_{i=1}^{n} f_i W^{(k)}(x_i) p_l^{(k)}(x_i) \end{aligned}\right\} \begin{array}{l} j, l = 0, 1, \ldots, M \\ r = 1, \ldots, N \end{array} \quad (13)$$

and

$$a^{(k)} := [a_0^{(k)}, a_1^{(k)}, \ldots, a_M^{(k)}]^T \quad (14)$$

$$b^{(k)} := [b_1^{(k)}, b_2^{(k)}, \ldots, b_N^{(k)}]^T \quad \text{and} \quad b_0^{(k)} := 1 \quad (15)$$

Using Eqns (3) and (6), Eqn (10) becomes

$$\sum_{i=1}^{n} W^{(k)}(x_i)[f_i Q^{(k)}(x_i) - P^{(k)}(x_i)] f_i q_r^{(k)}(x_i) = 0 \quad (16)$$

which, using Eqns (8) and (13), may be written as

$$E^{(k)} b^{(k)} = [C^{(k)}]^T a^{(k)} \quad (17)$$

where

$$E_{rs}^{(k)} := \delta_{rs} \sum_{i=1}^{n} f_i^2 W^{(k)}(x_i)[q_r^{(k)}(x_i)]^2 \quad r, s = 1, \ldots, N \quad (18)$$

Hence, eliminating $b^{(k)}$ from Eqn (12) using Eqn (17) yields the matrix equation

$$[D^{(k)} - C^{(k)}[E^{(k)}]^{-1}[C^{(k)}]^T]a^{(k)} = B^{(k)} \quad (19)$$

i.e. a linear system of dimension $(M + 1)$, in contrast with the original one of $(M + N + 1)$, Eqns (9) and (10). It should be noted that $E^{(k)}$ is a diagonal matrix and therefore has a very simple inverse. Finally, we note that the elements of the matrices $C^{(k)}$, $D^{(k)}$ and $E^{(k)}$ depend on the data (x_i, f_i) and the weight $W^{(k)} := [Q^{(k-1)}]^{-2}$.

In summary, the proposed method consists in the repeated construction and solution of the system of linear equations, given in Eqn (19) starting from a known $Q^{(0)}(x)$. Having computed the $a_j^{(k)}$ $(j = 0, 1, \ldots, M)$, Eqn (17) furnishes the $b_r^{(k)}$ $(r = 1, 2, \ldots, N)$. The coefficients $g_j^{(k)}$ and $h_j^{(k)}$ of x^j in each of the polynomials $P^{(k)}(x)$ and $Q^{(k)}(x)$, respectively, may now be determined and compared with those of the previous iteration, to determine whether or not convergence has been attained. Care must be taken to normalize these coefficients by ensuring that the leading coefficient of the denominator polynomial is unity. The iterations are continued until the following conditions are reached:

$$\max_{0 \leqslant j \leqslant M} |g_j^{(k)} - g_j^{(k-1)}| \leqslant \varepsilon \quad (20)$$

and

$$\max_{0 \leqslant r \leqslant N} |h_r^{(k)} - h_r^{(k-1)}| \leqslant \varepsilon \quad (21)$$

where ε (10^{-6}) is the tolerance set in the program.

Unlike polynomials, rational functions may exhibit infinite discontinuities in the region of interest. To check on the occurrence of such events, the zeros of the denominator can be inspected. Numerical experiments suggest that, if the degree of only one of the polynomials, numerator or denominator, is too large then the extra zero or pole usually lies outside the interval of approximation. Furthermore, if the degrees of both the numerator and denominator are greater than the optimal values then the excess zeros and poles often cancel each other. Thus, in a more general case than that dealt with in this paper, where the number of peaks is unknown, a comparison of the zeros of the numerator with those of the denominator can be used to help determine the optimum degrees for these polynomials.

Since each component in the spectrum corresponds to a quadratic factor of the denominator polynomial [cf. Eqn (1)], estimates of the position and width of a line may be determined from the real and imaginary parts, respectively, of the appropriate zeros of the denominator polynomials $(\alpha_k \pm j\beta_k, k = 1, \ldots, m)$.

Estimates of these complex zeros $(\bar{\alpha}_k \pm j\bar{\beta}_k, k = 1, \ldots, m)$ are provided by the NAG routine C02AGF. The fitted rational function may be written as

$$\frac{P(x)}{Q(x)} = \sum_{k=1}^{m} \left[\frac{a_k + jb_k}{x - (\bar{\alpha}_k + j\bar{\beta}_k)} + \frac{a_k - jb_k}{x - (\bar{\alpha}_k - j\bar{\beta}_k)} \right] \quad (22)$$

i.e.

$$\frac{P(x)}{Q(x)} = \sum_{k=1}^{m} \left[\frac{2a_k(x - \bar{\alpha}_k) - 2b_k\bar{\beta}_k}{(x - \bar{\alpha}_k)^2 + (\bar{\beta}_k)^2} \right] \quad (23)$$

for which it is readily shown that for the real numbers a_k, b_k

$$a_k + jb_k = \frac{P(\bar{\alpha}_k + j\bar{\beta}_k)}{Q'(\bar{\alpha}_k + j\bar{\beta}_k)} \quad k = 1, \ldots, m \quad (24)$$

where $Q'(x)$ denotes the first derivative, with respect to x, of the polynomial $Q(x)$. In this presentation it is assumed that the zeros of $Q(x)$ are simple.

In order to perform the necessary computations in real arithmetic, the real and imaginary parts of $P(\bar{\alpha}_k + j\bar{\beta}_k)$ are denoted by $P_R^{(k)}$ and $P_I^{(k)}$ respectively. A similar notation is used for $Q'(\bar{\alpha}_k + j\bar{\beta}_k)$. Hence,

$$a_k = \frac{P_R^{(k)}Q_R'^{(k)} + P_I^{(k)}Q_I'^{(k)}}{\Delta_k} \quad (25)$$

$$b_k = \frac{P_I^{(k)}Q_R'^{(k)} - P_R^{(k)}Q_I'^{(k)}}{\Delta_k} \quad (26)$$

where $\Delta_k = [Q_R'^{(k)}]^2 + [Q_I'^{(k)}]^2$ for $k = 1, \ldots, m$.

The real and imaginary parts of a polynomial may be calculated using the polar form of the zeros, i.e. $\bar{\alpha}_k + j\bar{\beta}_k = R_k \exp(j\theta_k)$. For example, if $Q(x) = \sum_{r=0}^{N} h_r^{(k)}x^r$, then

$$Q_R'^{(k)} = \sum_{r=0}^{N} r h_r^{(k)} R_k^{r-1} \cos[(r-1)\theta_k] \quad (27)$$

Horner's rule is then used to evaluate the polynomials.[11]

In this way, a partial fraction expansion with quadratic denominators is used to separate resonances which overlap. The intensities of the underlying Lorentzian lines are then given by

$$\lim_{a \to \infty} \int_{\bar{\alpha}_k - a}^{\bar{\alpha}_k + a} \frac{2a_k(x - \bar{\alpha}_k) - 2b_k\bar{\beta}_k}{(x - \bar{\alpha}_k)^2 + (\bar{\beta}_k)^2} \, dx = -2\pi b_k \quad (28)$$

for $k = 1, \ldots, m$.

The numerical stability of this method may be measured by the condition number, $\kappa(M)$ of the square matrix, M, say, on the left-hand side of Eqn (19). $\kappa(M)$ is defined by

$$\kappa(M) := \|M\| \|M^{-1}\| \quad (29)$$

where, in this paper, $\|M\|$ denotes the maximum row sum matrix norm,

$$\|M\| := \max_{0 \leqslant j \leqslant M} \sum_{r=0}^{M} |m_{jr}| \quad (30)$$

A detailed discussion of the role of condition number in estimating round-off error in the numerical solution of systems of linear equations is given in Ref. (12). In this work, $\kappa(M)$ is used simply as an indication of numerical stability. If $\kappa(M)$ is near unity then M is said to be well conditioned. However, if $\kappa(M)$ is 'significantly' greater than unity then the matrix M may be ill-conditioned. This depends on machine precision, which is about 10^{-15} in our case (e.g. double precision on a SUN Sparcstation as used in this work). If $\kappa(M)$ is expressed

in the form 10^q and if Gaussian elimination is used to solve Eqn (19) the resulting solution has about $(15 - q)$ correct significant figures. That is, about q significant figures have been lost due to round-off error. 'Well conditioned' in this instance refers to the relative security that a small residual vector implies a correspondingly accurate approximate solution. This measure is not precisely defined as it depends upon the machine accuracy of the computer in use. For the same machine, the lower the value of the condition number, the more accuracy (significant digits) can be obtained in the solution.

APPLICATION TO THREE-SPIN (1/2, 1/2, 1/2) SYSTEM

The isopropyl group of cholesterol is shown in Fig. 1 where, for simplicity in the following equations, carbon atoms C-25, C-26 and C-27 are labelled C_1, C_2 and C_3, respectively.

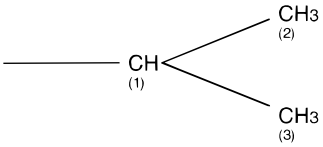

Figure 1. Isopropyl group of cholesterol.

The spin Hamiltonian operator for the above three-spin system[13] is

$$H = -\hbar B_0(\gamma_1 I_{1z} + \gamma_2 I_{2z} + \gamma_3 I_{3z}) + h({}^1J_{12}\bar{\mathbf{I}}_1 \cdot \bar{\mathbf{I}}_2 + {}^2J_{23}\bar{\mathbf{I}}_2 \cdot \bar{\mathbf{I}}_3 + {}^1J_{31}\bar{\mathbf{I}}_3 \cdot \bar{\mathbf{I}}_1 \quad (31)$$

where $\hbar$ is Planck's constant (h) divided by 2π, $\mathbf{B}_0$ is the applied external magnetic induction along the z axis, ${}^kJ_{ij}$ ($i, j = 1, 2, 3$, $i \neq j$, $k = 1, 2$) are the spin(i) − spin(j) coupling constants in hertz, γ_i are the gyromagnetic ratios (rad s^{-1} T^{-1}) and $\bar{\mathbf{I}}_i$ are the nuclear spin operators.

For the proton decoupled NMR spectrum of [25,26,27-^{13}C]cholesterol, the number of observed resonances is less than that for the general ABC system,[14,15] since it can be reasonably assumed that, for the carbon–carbon coupling constants, ${}^2J_{23} = 0$ and ${}^1J_{12} = {}^1J_{31} = J$, say.

The derivation of the eigenvalues of H is given in Appendix B. The allowed NMR transitions in this three-spin system are given in Fig. 2, with the corresponding spectrum in Fig. 3 for a spectrometer operating frequency of 90 MHz. The fitting procedure is applied to the four resonances in the lower chemical shift (δ) region in Fig. 3.

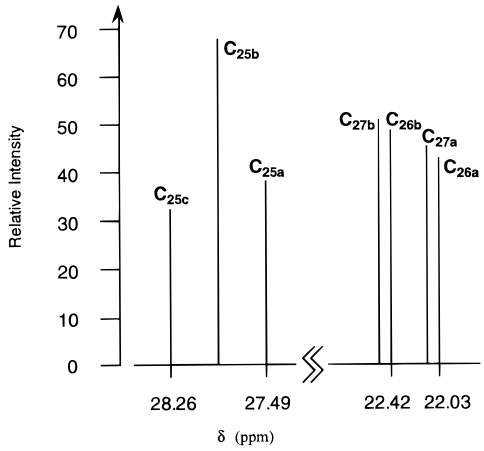

Figure 3. Theoretical calculated spectrum for C-25, C-26 and C-27 of 16.67 mol.% [25,26,27-^{13}C]cholesterol in DMPC vesicles at 90.56 MHz. The chemical shifts are with respect to TMS.

RESULTS

Figure 4(a)–(e) show the simulated symmetrical spectra under different spectrometer operating frequencies. The points in each simulated spectrum in these figures were determined using the experimentally measured coupling constants (J), chemical shifts and the relative intensity theoretically calculated from the transition probability matrix, with addition of 1% noise (i.e. S/N ratio of 100). The signal is defined as the maximum height of the underlying spectrum because the same simulated width has been used for each line. A total of 100 evenly spaced data points was used. The solid line represents the fitted lineshape obtained from the new method.

Experiments were carried out using different S/N ratios for each of the above overlapping lineshapes. Twelve parameters representing position, width and intensity were calculated for the four-resonances. The position of the C-26b resonance is used to illustrate the fitting procedure. The three-dimensional graph shown in Fig. 5 indicates the effects of the spectrometer oper-

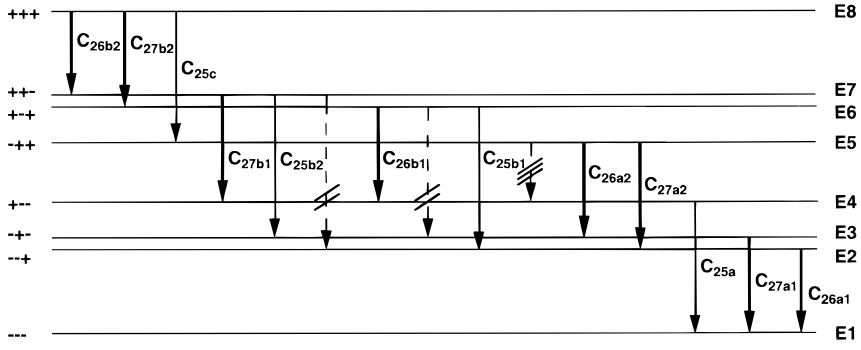

Figure 2. Energy level diagram with allowed NMR transitions for the three-spin (1-2, 1/2, 1/2) ABC system of [25,26,27-^{13}C]cholesterol. The energy level separations are not drawn to scale.

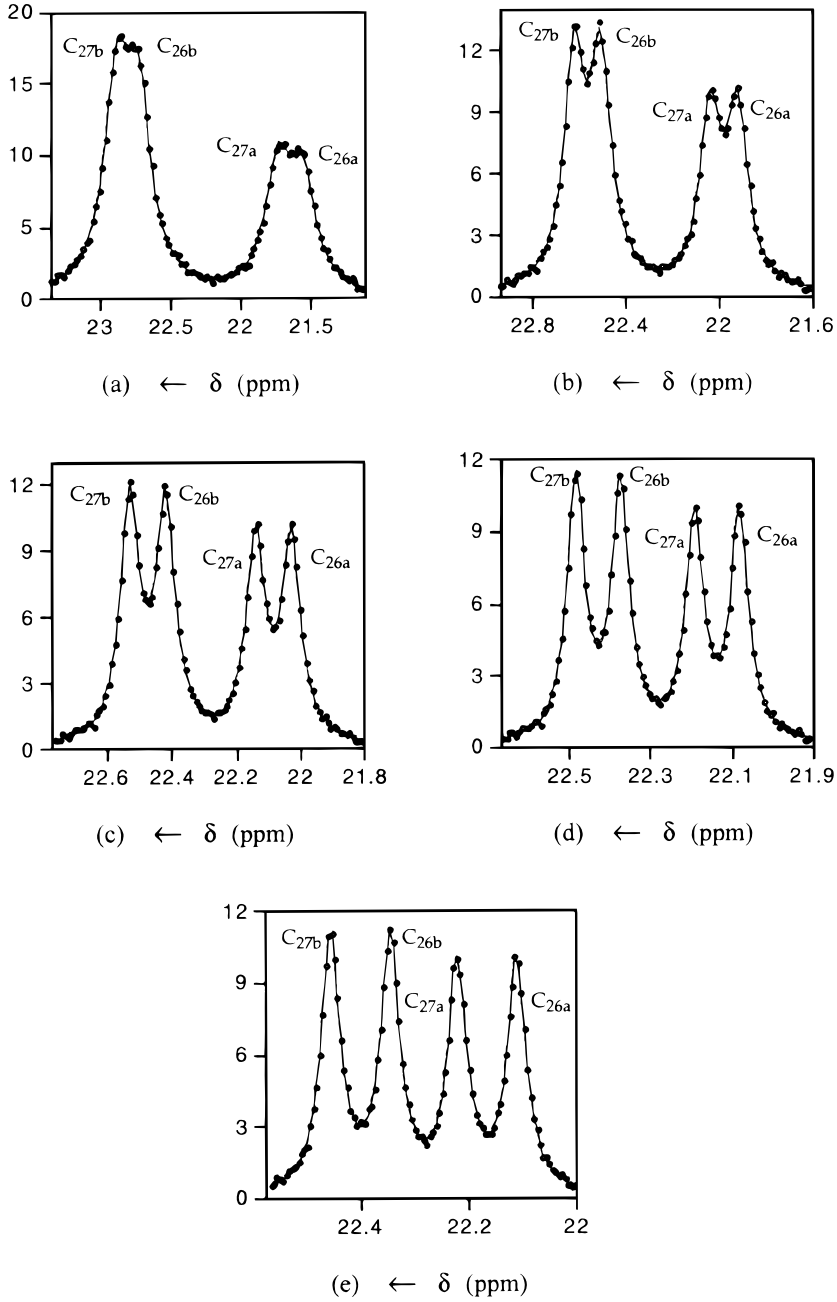

Figure 4. Simulated spectra for C-26 and C-27 of 16.67 mol.% [25,26,27-^{13}C]cholesterol in DMPC vesicles under different spectrometer operating frequencies: (a) 30; (b) 60; (c) 90; (d) 120; (e) 150 MHz.

ating frequency and S/N ratio on the accuracy of the calculated position parameter for the C-26b resonance. The ease of decomposition, describing the process of recovering the components from the spectroscopic data, depends on both the spectrometer operating frequency and S/N ratio. For example, the accuracy of simulation improves with an increase in the S/N ratio. The effects of the spectrometer operating frequency, however, are less straightforward. When the operating frequency is decreased, the overlap between the C-27a and C-26b resonances becomes weaker, while the overlap between the C-26a and C-27a and the C-26b and C-27b resonances, respectively, become stronger. For the extreme case of an operating frequency of 30 MHz, the spectrum appears as two well separated doublets with strong overlapping within each doublet. As shown in Fig. 5, the optimum operating frequency of 90 MHz results in the least relative percentage error in the C-26b position parameter. Similar graphs are obtained for all the other parameters. Under the same circumstances, the calculated position parameters are much more accurate (typically by a factor of 10) than the parameters for width and intensity.

At 30 MHz, an attempt was made to fit the two doublets independently using the same data as were used in the four-resonance fit. Regardless of the different S/N ratios, the fits always fail for the C-26a and C-27a doublet owing to severe overlapping unless the range used for fitting the above spectrum is restricted appropriately. Even then, the parameters are in some cases

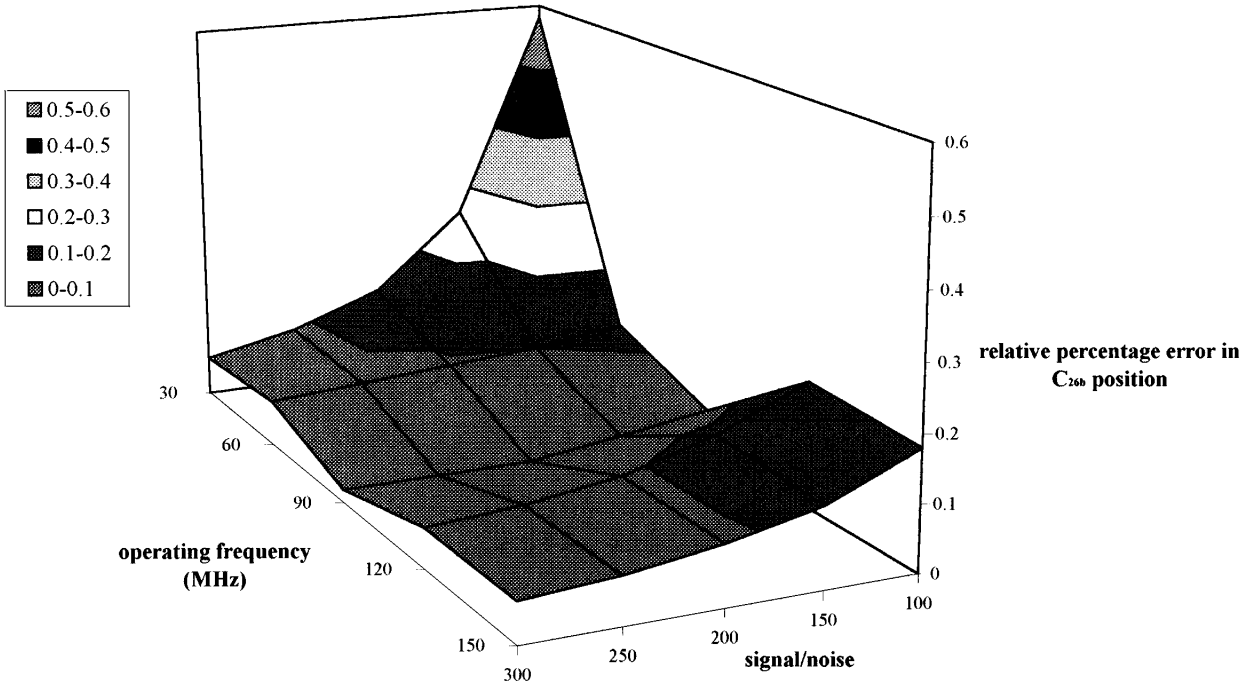

Figure 5. Effects of operating frequency and S/N ratio on simulation accuracy of the position of the C-26b resonance.

less accurate than those obtained from the four-resonance fit. In the case of the C-26b and C-27b doublet, a fit is always obtained regardless of range, but again the results are often less accurate than the case of the four-resonance fit. Unlike the four-resonance fit, the interference from one doublet is not included in the fitting of another doublet when applying the two-resonance fit twice. These results suggest that the new method is more robust for the four-resonance case than for the two-resonance case applied twice.

Comparison in terms of condition number with the direct application of rational functions without using orthogonal polynomials[8] for the four-resonance case is shown in Table 1. This indicates that a significant reduction in ill-conditioning is obtained by the use of orthogonal polynomials.

The characteristic sensitivity to pre-estimates of the standard non-linear least-squares procedure (i.e. NAG E04EDF) for a frequency of 90 MHz and an S/N ratio of 100 is shown in Fig. 6, where the two axes represent the pre-estimates of the position and width for the C-26b resonance. The other pre-estimates are fixed and are equal to the exact values of the underlying parameters. The largest solid circle indicates the exact underlying values of the two variables. The open circles represent inappropriate pre-estimates (those which lead to physically meaningless results), while appropriate pre-estimates are represented by the solid circles. Unless all the pre-estimates are close to the ultimate values, the least-squares fitting process may be very unpredictable. For example, when the position parameter is fixed at 22.4926, a width parameter of 0.0408 is a successful pre-estimate. Width values of 0.0458 and 0.0358, however, both lead to poor results. Similar results are obtained for the other cases. Moreover, the greater the overlapping of the lineshapes, the more sensitive is this stan-

Table 1. Comparison of condition numbers obtained from rational approximants with and without use of orthogonal polynomials (O.P.)[a]

S/N ratio	Without O.P.	With O.P.
100	1.5×10^{16}	4.2×10^{6}
150	1.6×10^{16}	5.2×10^{6}
200	1.4×10^{16}	5.6×10^{6}
250	1.9×10^{16}	5.7×10^{6}
300	1.6×10^{17} [b]	5.8×10^{6}

[a] Spectrometer operating frequency = 30 MHz.
[b] Results obtained before the execution is terminated.

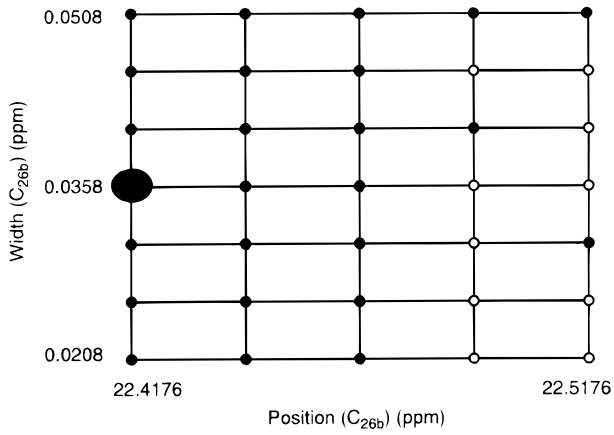

Figure 6. Sensitivity of the standard non-linear least-squares procedure to the pre-estimates of the position and width of the C-26b resonance. The solid and open circles indicate pre-estimates which led and failed to lead, respectively, to convergence of the fitting procedure. The large solid dot represents the exact value. The increments are 0.005 and 0.025 ppm on the vertical and horizontal scales, respectively.

dard method to pre-estimates. In fact, for each resonance, there are three pre-estimates to be determined. Therefore, for cases of more than two resonances, this unpredictability becomes complicated and it makes a proper selection of pre-estimates more difficult.

At 90 MHz, 100 sets of data for 100 different seeds were tested with an S/N ratio of 100. The average value of each of the 12 parameters obtained from these 100 data sets for both the standard non-linear least-squares procedure and the new approach are summarized in Table 2. The errors indicated from the former method are smaller than those from the new method for the tolerance used. This is a consequence of the slower convergence of the new method close to the exact values. Both methods take approximately the same time to execute, namely 1.3 and 0.8 s for the new and former methods, respectively. The new method typically used 20 iterations. Table 3 shows that the difference in the values of the coefficients of the starting polynomials and the fitted values from the new method are much larger than the initial and fitted values of the parameters (intensity, position and width) from the former method. This demonstrates that, in contrast to the former method, the initial values used for the new method are essentially arbitrary. The arbitrary nature of the initial values indicates the superior robustness of the new method compared with the former. It should be noted that pre-estimates for the numerator polynomial are not required in the new method. Hence, only eight starting values are required for the new method compared with 12 for the former method.

DISCUSSION

The new form of rational function described is well suited to fitting overlapping resonance lines of a Lorentzian shape. For the example examined of four overlapping resonances, this method is more robust than that previously described where the spectrum may be considered as two doublets which are fitted independently. By using rational functions based on sets of orthogonal polynomials, the condition number is greatly reduced, compared with the standard choice of

Table 2. Averages of parameter values for both the standard non-linear least-squares procedure and the new approach from 100 sets of data with S/N = 100 (positions and widths are given in ppm)

Parameters	Species	Exact value	Standard procedure	New approach
Intensities	C-26a	1.007	1.015 ± 0.023	0.999 ± 0.037
	C-27a	1.023	1.010 ± 0.023	1.029 ± 0.042
	C-26b	1.228	1.196 ± 0.024	1.230 ± 0.036
	C-27b	1.210	1.228 ± 0.024	1.200 ± 0.028
Positions	C-26a	22.0293	22.0279 ± 0.0005	22.0361 ± 0.03
	C-27a	22.1401	22.1388 ± 0.0007	22.1306 ± 0.03
	C-26b	22.4165	22.4177 ± 0.0005	22.4170 ± 0.001
	C-27b	22.5272	22.5283 ± 0.0005	22.5290 ± 0.001
Widths	C-26a	0.035575	0.0358 ± 0.0011	0.0357 ± 0.0013
	C-27a	0.035575	0.0358 ± 0.0010	0.0368 ± 0.0017
	C-26b	0.035575	0.0357 ± 0.0008	0.0371 ± 0.0011
	C-27b	0.035575	0.0358 ± 0.0008	0.0354 ± 0.0001

Table 3. Example to show the insensitivity of the fit for the new method over the standard non-linear least-squares procedure (positions and widths are given in ppm)

		Standard method			New method			
Parameter	Species	Pre-estimate	Fit	Difference	Coefficient of denominator	Starting values ($k = 0$)	Fit ($k = k_{max}$)	Difference
Intensity	C-26a	0.0015	0.0122	0.0003	$h_0^{(k)}$	1.0	0.0125	0.9875
	C-27a	0.0015	0.0113	0.0002	$h_1^{(k)}$	1.0	−0.0256	1.0256
	C-26b	0.0136	0.0133	0.0003	$h_2^{(k)}$	1.0	0.02218	0.7782
	C-27b	0.0139	0.0135	0.0004	$h_3^{(k)}$	1.0	−1.0680	2.0680
Position	C-26a	22.0280	22.0286	0.0006	$h_4^{(k)}$	1.0	3.1199	2.1199
	C-27a	22.1388	22.1385	0.0003	$h_5^{(k)}$	1.0	−5.6617	6.6617
	C-26b	22.3176	22.4176	0.1000	$h_6^{(k)}$	1.0	6.2395	5.2395
	C-27b	22.5283	22.5285	0.0002	$h_7^{(k)}$	1.0	−3.8242	4.8242
Width	C-26a	0.0358	0.0367	0.0009	$h_8^{(k)}$	1.0	1.0	0
	C-27a	0.0358	0.0359	0.0001	—	—	—	—
	C-26b	0.0458	0.0350	0.0108	—	—	—	—
	C-27b	0.0358	0.0351	0.0007	—	—	—	—

polynomials. This decrease in the condition number is an indication of the improvement in the numerical stability of the method.

A main advantage of this approach is robustness, i.e. the insensitivity of the fit to the choice of starting values for the resonance parameters. Since the choice of starting values is essentially arbitrary [e.g. $Q^{(0)}(x) = 1 + x + x^2 + \cdots + x^N$], this method could be used to provide suitable starting values for a subsequent fitting procedure. This method is particularly well suited to accurate determination of the positions of overlapping resonances with good S/N ratios. As with other methods, the ability to fit overlapping resonance peaks decreases as the S/N ratio decreases.

REFERENCES

1. H. Barkhuijsgen, R. De Beer and D. Van Ormondt, *J. Magn. Reson.* **73**, 553 (1987).
2. S. Van Huffel, H. Chen, C. D. Decanniere and P. Van Hecke, *J. Magn. Reson. A* **110**, 228 (1994).
3. W. H. Press, B. P. Flannery, S. A. Teukolsky and W. T. Vetterling, *Numerical Recipes in Pascal*, p. 574. Cambridge University Press, Cambridge (1989).
4. J. Cao, *J. Magn. Reson. B* **103**, 296 (1994).
5. F. D. Rio-Portilla, V. Blechta and R. Freeman, *J. Magn. Reson. A* **111**, 132 (1994).
6. Y. L. Martin., *J. Magn. Reson. A* **111**, 1 (1994).
7. M. M. Maltempo, *J. Magn. Reson.* **68**, 102 (1986).
8. G. Bergmann, W. Dietrich, U. Günther and W. M. Wiecken, *J. Magn. Reson.* **76**, 193 (1988).
9. J. Higinbotham, P. H. Beswick, R. J. Malcolmson, D. Reed, J. A. Parkinson and I. H. Sadler, *Chem. Phys. Lipids*, **66**, 1 (1993).
10. R. Yusaf, personal communication.
11. A. Ralston and P. Rabinowitz, *A First Course in Numerical Analysis*, p. 287. McGraw-Hill, Singapore (1984).
12. G. H. Golub and C. F. Van Loan, *Matrix Computations*. John Hopkins University Press, Baltimore (1989).
13. C. P. Poole and H. A. Farach, *Theory of Magnetic Resonance*, 2nd ed., p. 80. Wiley, New York (1987).
14. J. A. Pople, W. G. Schneider and H. J. Bernstein, *High Resolution Nuclear Magnetic Resonance*, pp. 27, 130. McGraw-Hill, New York (1959).
15. F. A. Bovey, L. Jelinski and P. A. Mirau, *Nuclear Magnetic Resonance Spectroscopy*, 2nd ed., p. 175. Academic Press, London (1988).

APPENDIX A

Orthogonal polynomials with respect to a weight function

It is required to construct polynomials $p_j(x)$ each of degree j, for $j = 0, 1, \ldots$, orthogonal over the given set of points $(x_1, x_2, \ldots, x_n)$ with respect to a given weight function $W(x)$ [$W(x_i) > 0$ for all x_i, $i = 1, 2, \ldots, n$], i.e.

$$\sum_{i=1}^{n} W(x_i) p_j(x_i) p_l(x_i) = \lambda_j \delta_{jl} \tag{A1}$$

where $\lambda_j > 0$. This is achieved using the recurrence relation

$$p_{j+1}(x) = (x - \rho_{j+1}) p_j(x) - \sigma_j p_{j-1}(x) \quad j = 0, 1, \ldots \tag{A2}$$

with the initialization $p_{-1}(x) \coloneqq 0$, $p_0(x) \coloneqq 1$. The parameters ρ_{j+1} and σ_j are defined at each stage by

$$\rho_{j+1} \coloneqq \sum_{i=1}^{n} W(x_i) x_i [p_j(x_i)]^2 \Big/ \sum_{i=1}^{n} W(x_i) [p_j(x_i)]^2 \tag{A3}$$

$$\sigma_j \coloneqq \sum_{i=1}^{n} W(x_i) [p_j(x_i)]^2 \Big/ \sum_{i=1}^{n} W(x_i) [p_{j-1})[x_i)]^2 \tag{A4}$$

A derivation of this result was given by Ralston and Rabinowitz.[11]

APPENDIX B

Calculation of energy levels and transition probabilities for the three-spin (1/2, 1/2, 1/2) ABC system

The spin Hamiltonian operator for a scalar-coupled ABC system with isotropic chemical shift interaction[13] is given by Eqn (21)]. The matrix of this Hamiltonian in the product basis was given by Poole and Farach.[13]

The eigenvalues of the lowest and the highest energy levels are

$$E_1 = \hbar[-B_0(\gamma_1 + \gamma_2 + \gamma_3) + 2\pi J]/2 \tag{B1}$$

$$E_8 = \hbar[B_0(\gamma_1 + \gamma_2 + \gamma_3) + 2\pi J]/2 \tag{B2}$$

The remaining six eigenvalues result from the solutions of two cubic equations. Using the assumptions described in Eqns (22) and (23), these simplify to give the following solutions:[A1]

$$E_2 = \hbar\{p \cos[(\cos^{-1} q)/3] - t_1/3\}/2 \tag{B3}$$

$$E_3 = \hbar\{p \cos[(\cos^{-1} q)/3 + 2\pi/3] - t_1/3\}/2 \tag{B4}$$

$$E_4 = \hbar\{p \cos[(\cos^{-1} q)/3 + 4\pi/3] - t_1/3\}/2 \tag{B5}$$

where

$$p = \sqrt{\frac{4|t_2 - {t_1}^2/3|}{3}} \tag{B6}$$

$$q = \frac{4}{3p^3}(t_1 t_2 - 3t_3 - \tfrac{2}{9}{t_1}^3) \tag{B7}$$

and

$$t_1 = B_0(\gamma_1 + \gamma_2 + \gamma_3) + 2\pi J \quad \text{(B8)}$$

$$t_2 = -B_0{}^2(\gamma_1{}^2 + \gamma_2{}^2 + \gamma_3{}^2 - 2\gamma_1\gamma_2 - 2\gamma_2\gamma_3 - 2\gamma_3\gamma_1) + 4\pi B_0\gamma_1 J - 8\pi^2 J^2 \quad \text{(B9)}$$

$$t_3 = B_0{}^2[\gamma_1{}^2 - (\gamma_2 - \gamma_3)^2][B_0(\gamma_2 + \gamma_3 - \gamma_1) + 2\pi J] - 8\pi^2 B_0\gamma_1 J^2 \quad \text{(B10)}$$

Similarly, E_5, E_6 and E_7 are given by

$$E_5 = \hbar\{u\cos[(\cos^{-1} v)/3] - s_1/3\}/2 \quad \text{(B11)}$$

$$E_6 = \hbar\{u\cos[(\cos^{-1} v)/3 + 2\pi/3] - s_1/3\}/2 \quad \text{(B12)}$$

$$E_7 = \hbar\{u\cos[(\cos^{-1} v)/3 + 4\pi/3] - s_1/3\}/2 \quad \text{(B13)}$$

where

$$u = \sqrt{\frac{4|s_2 - s_1{}^2/3|}{3}} \quad \text{(B14)}$$

$$v = \frac{4}{3u^3}(s_1 s_2 - 3s_3 - \tfrac{2}{9}s_1{}^3) \quad \text{(B15)}$$

and

$$s_1 = -B_0(\gamma_1 + \gamma_2 + \gamma_3) + 2\pi J \quad \text{(B16)}$$

$$s_2 = -B_0{}^2(\gamma_1{}^2 + \gamma_1{}^2 + \gamma_3{}^2 - 2\gamma_1\gamma_2 - 2\gamma_2\gamma_3 - 2\gamma_3\gamma_1) - 4\pi B_0\gamma_1 J^2 - 8\pi^2 J^2 \quad \text{(B17)}$$

$$s_3 = B_0{}^2[\gamma_1{}^2 - (\gamma_2 - \gamma_3)^2][B_0(\gamma_1 - \gamma_2 - \gamma_3) + 2\pi J] + 8\pi^2 B_0\gamma_1 J^2 \quad \text{(B18)}$$

The corresponding eigenfunctions are used to obtain the transition probability matrix elements[14] between these energy levels. There are 28 possible transitions but 13 of them have matrix elements which are identically zero. Of the remaining 15, three (7–2, 6–3 and 5–4) have negligibly small elements. The frequencies of the remaining 12 transitions are shown in Fig. 2. For example,

$$\omega_{25a} = (E_4 - E_1)/\hbar \quad \text{(B19)}$$

The relative intensity of a transition $E_i \rightarrow E_j$ is obtained from the square of the corresponding transition elements.

The allowed NMR transitions in this three-spin system are indicated in Fig. 2. The 12 transitions include five pairs of doublets, the components of which are too close to be resolved. Fig. 3 shows the calculated positions and intensities of the remaining seven lines in the spectrum for the particular isopropyl three spin-1/2 ABC system used in this study, for a spectrometer operating frequency of 90.56 MHz.

The fitting procedure is applied to the four resonances shown in the lower chemical shift range of Fig. 3.

REFERENCE

A1. G. Birkhoff and S. MacLane, *A Survey of Modern Algebra*, 2nd ed., p. 112. Macmillan, New York (1953).